# Self-Organized Stationary Patterns in Networks of Bistable Chemical Reactions

Nikos E. Kouvaris,[1,*] Michael Sebek,[2] Alexander S. Mikhailov,[3] and István Z. Kiss[2]

[1] *Department of Physics, University of Barcelona, Martí i Franquès 1, 08028 Barcelona, Spain*
[2] *Department of Chemistry, Saint Louis University, 3501 Laclede Ave., St. Louis, Missouri 63103, USA*
[3] *Department of Physical Chemistry, Fritz Haber Institute of the Max Planck Society, Faradayweg 4-6, D-14195 Berlin, Germany*

(Dated: September 27, 2016)

Theoretical investigations of networks of diffusively coupled bistable elements have shown that they can support stationary self-organized activity patterns. Here, we report the results of experiments with networks of coupled electrochemical bistable elements that not only confirm such theoretical predictions, but also prove their high robustness. In the experiments, networks with various topologies (i.e., regular and irregular trees) could be constructed by locally coupled electrochemical units with bistable individual dynamics. By applying initial activation to different (subsets of) nodes in such networks, we could observe subsequent spreading or retraction of activation over the networks and formation of different stationary activity patterns. The final stationary patterns depended sensitively on the architecture of the networks and the initial conditions. The agreement with the theoretical predictions was excellent, even though the bistable dynamics of electrochemical elements was based on a complex, and not yet completely known, mechanism and the local coupling between the elements in a network was not strictly diffusional.

arXiv:1609.07783v1 [nlin.PS] 25 Sep 2016

## I. INTRODUCTION

Complex networks can be formed by chemical reactors [1–3], biological cells [4], or engineered units [5–7]. An interplay between local dynamics at the nodes and architecture of the links in such systems leads to a wealth of self-organization phenomena, including synchronization [3, 8, 9], stationary Turing and oscillatory patterns [10–14], or excitation waves [15–17]. The Turing mechanism [18] requires a difference in diffusion rates of inhibitor and activator species, which destabilizes a spatially homogeneous steady state and gives rise to the formation of new spatial patterns [19, 20]. Here, an alternative mechanism for emergence of stationary patterns in networks of coupled bistable units is experimentally explored. Bistable units can be found in a broad class of chemical reactions, see e.g. [21], but also in cellular [22], social [23], and engineered systems [24]. Such units can have local or diffusive connections between them.

In continuous bistable media, traveling or retreating activation fronts are observed [25]. In chains and lattices of diffusively coupled one-component bistable elements, traveling fronts can become pinned if coupling is sufficiently weak [26–29] and thus stationary patterns are formed. Recently, the theory has been extended to networks representing trees and a rich variety of stationary patterns, sensitive to the topology of the networks, has been predicted [30, 31]. However, experimental confirmation of the theory has been so far missing. Now, in the experiments with specially constructed tree networks of electrochemical units, we not only confirm the theoretical predictions, but also show that they hold well beyond the simplifying conditions under which the theory has been developed.

## II. THEORY OF BISTABLE TREE NETWORKS

Suppose that some substance can undergo chemical reactions in reactors occupying nodes $i$ $(i = 1, \ldots, N)$ of a network and this substance can spread diffusively from one node to another. Such a network-organized reaction-diffusion system is generally described by equations

$$\dot{u}_i = f(u_i) + K \sum_{j=1}^{N} (A_{ij} u_j - A_{ji} u_i) \,, \qquad (1)$$

where $u_i$ is the chemical concentration in the node $i$, the function $f(u)$ specifies the local dynamics at the nodes, and the coefficient $K$ characterizes the strength of diffusive coupling. The function $f(u)$ can be chosen in such a way that individual elements are bistable. In our theoretical analysis, we employed a classical one-component bistable system [32] to describe the dynamics in the network nodes. Specifically, the dynamics was characterized by the cubic function

$$f(u) = -u(u-h)(u-a) \,, \qquad (2)$$

where $u$ represented the chemical concentration in a node. Function $f(u)$ had three roots which corresponded to the fixed points of the local dynamics: two stable fixed points with real negative eigenvalues (i.e., stable nodes) at $u = 0$ and $u = a$, and one unstable fixed point with two real eigenvalues of opposite signs (i.e., a saddle point) at $u = h$.

The network structure is determined by a symmetric adjacency matrix whose elements are $A_{ij} = 1$, if there is a connection between nodes $i$ and $j$ $(i \neq j)$, and $A_{ij} = 0$

*Electronic address: nkouba@gmail.com

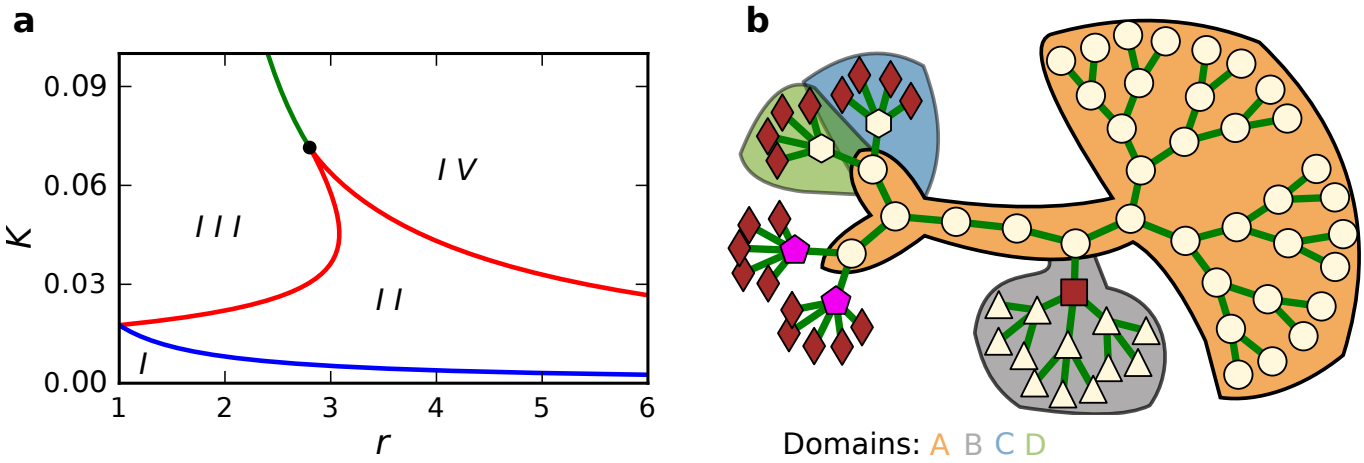


FIG. 1: Analytical theory and numerical simulations. **a,** The bifurcation diagram: Region $I$: Center and periphery activations are pinned. Region $II$: Center activation is pinned whereas periphery activation propagates towards the center of the tree. Region $III$: Center and periphery activations propagate in both directions, to the periphery and the center of the tree. Region $IV$: Center activation retreats whereas periphery activation propagates towards the center of the tree. **b,** Different activity domains in a non-regular tree network. Active domains $A$, $B$, $C$, and $D$, are distinguished by different colors. Activation of any node with the cream color (○, △, ⬡) results in spreading of the activation over all nodes in the respective network domains $A$, $A \cup B$, $A \cup C$, or $A \cup D$. Activation of any node with the brown color (□, ♢) remains pinned on that node. Activation of a single node with the magenta color (⬠) retreats and vanishes resulting in the uniform passive state. The parameters are $h = 0.245$, $a = 1$ and $K = 0.04$.

otherwise. For such models an approximate analytical theory is available [30] for special networks representing regular trees. In a regular tree with the branching ratio $r$, each node in the layer $l$ is connected to $r$ nodes in the next layer $l+1$ and dynamics can be described by equations

$$\dot{u}_l = f(u_l) + K[u_{l-1} - (r+1)u_l + r u_{l+1}]\,, \qquad (3)$$

where $u_l$ is the chemical concentration in the layer $l$. Previously, it was theoretically shown [30] that such equations support traveling and pinned (stationary) fronts, and the transition between them occurs via saddle-node bifurcations. Here we determine these bifurcations as a function of the parameters $r$ and $K$. In the parameter plane $r - K$ (see FIG. 1a), fronts which correspond to center activation get pinned via a saddle-node bifurcation at

$$\begin{aligned} r &= \frac{(2u-h)(a-u)^2}{(a+h-2u)u^2}\,, \\ K &= \frac{(a+h-2u)u^2}{a} \end{aligned} \qquad (4)$$

(red curves) and merge in the cusp point

$$(r, K) = \left(\frac{(2a-h)^3}{(a+h)^3}, \frac{(a+h)^3}{27a}\right) \qquad (5)$$

(black point). They separate regions $II$ (pinned, stationary fronts) from region $III$ (propagating fronts) as well as region $II$ from region $IV$ (retreating fronts). Fronts can also turn from propagating to retreating ones without getting pinned, when the curve

$$K = \frac{(a-2h)(2a-h)(a+h)}{9[h-2a+(h+a)r]} \qquad (6)$$

(green curve that separates regions $III$ and $IV$) is traversed. Fronts that correspond to peripheral activation get pinned via a saddle-node bifurcation at

$$\begin{aligned} r &= \frac{(a+h-2u)u^2}{(2u-h)(a-u)^2}\,, \\ K &= \frac{(2u-h)(a-u^2)}{a} \end{aligned} \qquad (7)$$

(blue curve). While they are pinned in region $I$, the fronts begin to propagate towards the center of the tree when the bifurcation boundary is crossed. Peripheral activation cannot retreat. The bifurcation diagram in FIG. 1a is drawn for the parameter values $a = 1$ and $h = 0.245$.

The analytical and numerical results are summarized in FIG. 1. Under given nonlinearity factors (that determine the range of bistability and the transition boundary between the two stable states), the two major parameters are the coupling strength ($K$) and the branching ratio of the regular tree ($r$). For weak coupling, the activation is pinned (i.e., it does not propagate) in region $I$. At the intermediate coupling strength there is a range of branching ratios (region $II$), where the center

activation is pinned while the periphery activation propagates towards the center. At sufficiently strong coupling and relatively low branching ratios (region $III$), the center activation spreads towards to periphery, whereas the periphery activation propagates towards the center. At strong coupling and large branching ratios (region $IV$), the center activation retreats and the periphery activation propagates towards the center. The behavior of a regular tree with a fixed branching ratio can be fully interpreted in terms of these four regimes. Moreover, these results can also be applied to analyze the behavior in more complex, non-regular tree networks.

Figure 1b shows a non-regular tree network with branching ratios varying from one or two (domain $A$), three (domain $B$), four (domain $C$) and five (domain $D$). Numerical simulations for this network were performed with the coupling constant $K = 0.04$, so that these domains corresponded to regions $II$, $III$ or $IV$ in the bifurcation diagram. Simulations were done by applying initial activation to one of the nodes and following the subsequent evolution until a stationary state was reached. Stationary patterns were then classified by identifying all the possible stationary states that could be obtained by such an initial activation.

The developed patterns can be interpreted by the formation of domains activated individually or in combinations. The domains consist of groups of nodes that correspond to the same dynamical region and thus behave similarly. For example, domains of elements in region $III$ support spreading of activation towards both the center and the periphery. When such domains are adjacent to, or surrounded by nodes that are amenable to pinning or to retreating (e.g., in region $I$, $II$, or $IV$), the propagating fronts get pinned and stationary structures develop. Therefore, the observed structures consist of uniform domains separated by nodes amenable to pinning or to retreating. The exact configuration of the patterns depends on the architecture of the network, the applied coupling strength, and the nonlinearity of the reaction that altogether determine the assignment of the nodes to the different regions and the configuration of the domains.

For the specific network, shown in FIG. 1b, activation of a node with the cream color resulted in spreading of activation to all nodes of the domains $A$, $A \cup B$, $A \cup C$, or $A \cup D$. Activation of a node with the brown color remained pinned on that node. Activation of a node with the magenta color retreated and vanished resulting in the uniform final passive state. Simulations were also performed by initially activating several network nodes, but essentially the same final patterns were then reached.

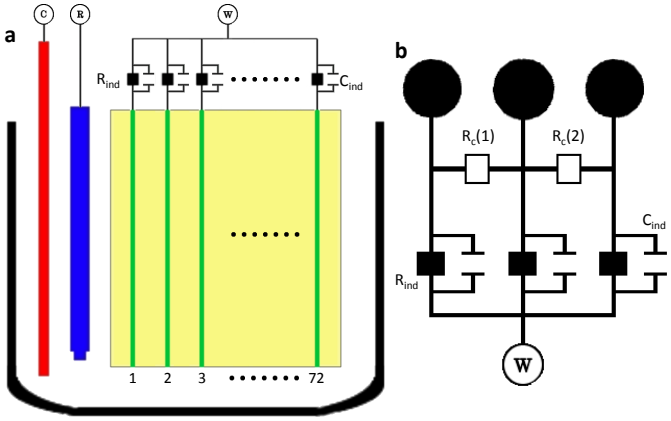


FIG. 2: Experimental apparatus and electric diagram. **a,** The experimental setup: $C$ is counter electrode, $R$ is reference electrode and $W$ is the working electrode array. There are 72 electrodes in the electrode array each has an $R_{\rm ind}$ and $C_{\rm ind}$ in parallel. **b,** The electric diagram: The black circles are the electrodes which connect to the working point through parallel $R_{\rm ind}$ and $C_{\rm ind}$. The empty boxes are $R_{\rm c}$ where $R_{\rm c}(1)$ connects the first to the second electrode and $R_{\rm c}(2)$ connects the second to the third electrode. Similarly, the connection may be non-local by connecting a coupling resistance between two non-local electrodes.

## III. EXPERIMENTAL OBSERVATION OF STATIONARY DOMAINS IN ELECTROCHEMICAL BISTABLE NETWORKS

Experiments with networks of bistable electrochemical reactions were performed. Each element (see FIG. 2) represented a corroding metal (nickel) wire that accommodated a complex reaction system (including, e.g., formation of multiple forms of metal oxides, bisulfate adsorption, oxygen evolution and metal dissolution) that exhibited bistable behavior. Moreover, coupling was established in the form of the charge flow between the wires (due to difference in electrode potential) which affected the rate of metal dissolution of the coupled electrodes.

### A. Experimental apparatus

We performed experiments using an electrochemical cell where a platinum coated titanium rod is the counter electrode, $Hg/Hg_2SO_4$/saturated $K_2SO_4$ is the reference electrode, an electrode array of 72 nickel, 1.00 mm diameter, wires embedded in epoxy is the working electrode and the electrolyte is 3M $H_2SO_4$ (Macron Chemicals, Lot# K39005) held at 10 °C. Each electrode in the array is connected to a potentiostat (ACM Instruments GillAC) through an individual resistance ($R_{\rm ind}$) of 1 $k\Omega$ and an individual capacitance ($C_{\rm ind}$) of 4.7 $mF$ in parallel (see FIG. 2a). We apply a constant circuit potential ($V$) and the current of each electrode in the array is measured at 50 $Hz$. All electrodes exhibit bistability for a range of

circuit potential $[V_{\min}, V_{\max}]$. The $C_{\text{ind}}$ serves to prevent the oscillations which naturally occur at the applied potential region of interest. For each experiment, we set the circuit potential $V$ such that $V = V_{\min} + (V_{\max} - V_{\min})/4$; this procedure ensures that the dynamics is similar in the repeated experiments. Desired active (high current) or passive state (low current) is achieved by superimposing a locally applied potential sweep on the circuit potential.

Interactions between electrodes occur through external resistance connections. The strength of the interactions are controlled by the coupling resistance ($R_c$); the coupling strength ($K$) is the inverse of $R_c$. When the electrodes are connected, a network topology, determined by the external connections, is established. Electrodes are the nodes and the external connections are the links between nodes in all network diagrams. A simple three electrode schematics is shown in FIG. 2b where the electrodes are coupled linearly.

Bistable region is not exactly the same for every electrode, therefore the experimental results exhibit some minor deviation from numerical simulations and theoretical predictions.

### B. Experimental results

It should be noted that, although our experimental systems indeed represented a network of coupled bistable elements, it was not accurately described by a simple one-component model used in the theoretical analysis. A realistic quantitative model for such electrochemical elements is not yet available, but it should definitely include many chemical variables. While coupling was pairwise, it could not be interpreted as corresponding to diffusion of a certain chemical species. Because of such differences, the validity of theoretical predictions was not obvious.

First, experiments with regular trees were undertaken. Figure 3 shows that center activation in a four-layer tree with the branching ratio 3 could result in spreading fronts (FIG. 3b, region $III$) for weak coupling, pinned fronts (FIG. 3c, region $II$) for moderate coupling, and retreating fronts (FIG. 3d, region $IV$) for strong coupling. Similarly, periphery activation (FIG. 3e) yielded either pinned fronts (FIG. 3e, region $I$) at very weak coupling or spreading fronts (FIG. 3f) at stronger coupling; such behavior was found in all regions II, III, or IV.

Figure 4 shows the evolution observed in the same network after activation of an intermediate node at different coupling strengths. In region $I$ (FIG. 4a) the fronts are pinned on both sides. In region $II$ (FIG. 4b) the center facing front spreads towards the center and the periphery facing front is pinned. In region $III$ fronts spread in both directions and finally activate the entire network (FIG. 4c). In region $IV$ the center facing front propagates towards the center but the periphery facing front is retreated from the periphery finally establishing the passive state in the entire network (FIG. 4d). All these experiments confirm the theoretical predictions for the regular tree networks.

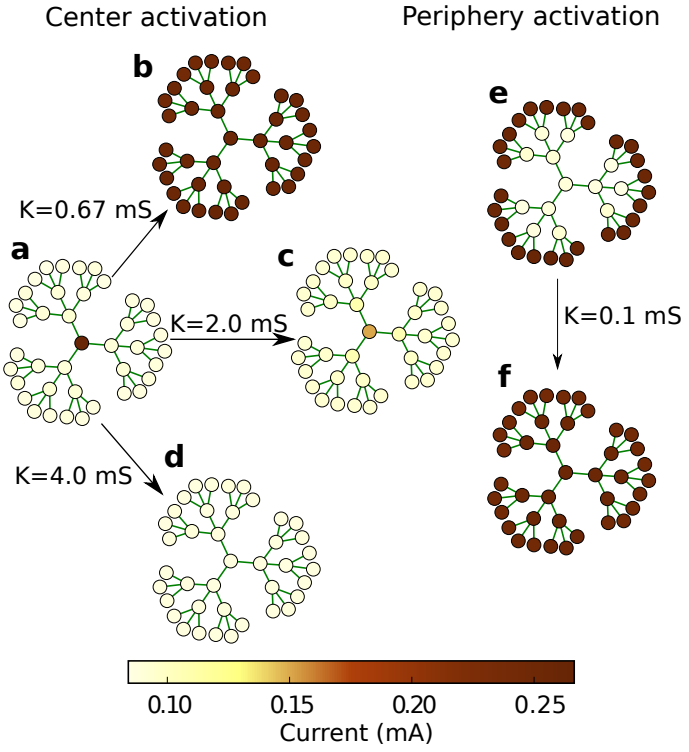


FIG. 3: Experiments with regular trees: Center and periphery activation. Evolution of center and periphery activations on a regular tree with the branching ratio $r = 3$ at different coupling strengths $K$. **a,** Initial condition of center activation. **b,** Spreading front, $K = 0.67\ mS$; final state at $t = 1008\ s$ is shown. **c,** Pinned front, $K = 2.0\ mS$, $t = 2310\ s$. **d,** Retreating front, $K = 4.0\ mS$, $t = 68\ s$. **e,** Initial condition of periphery activation. If $K = 0.04\ mS$ the front is pinned, $t = 480\ s$. **f,** Spreading front, $K = 0.10\ mS$, $t = 464\ s$. $V = 1300mV$; color coding indicated by the bar is used to display currents in network nodes.

Furthermore, we could also build the same non-regular tree as in the simulations in FIG. 1b. By performing experiments with regular trees under the same experimental setup, we could find (see Supplemental Figure S1) that at $K \approx 1\ mS$ regions $II$, $III$, and $IV$ correspond to the branching ratios $r = 3,\ 4$, $r = 1,\ 2$, and $r \geq 5$, respectively. Similar to theoretical predictions, we could see that activations with a single (FIG. 5a and Supplemental Video S1) or multiple nodes (FIG. 5b and Supplemental Video S2) within domain $A$ resulted in activation of all elements in domain $A$. When activation was applied to an intermediate element of domain $B$, pattern $A \cup B$ was observed (FIG. 5c and Supplemental Video S3). To achieve complete activation of the network, peripheral nodes of the branches with the highest branching ratios $r = 3,\ 4$ and 5 had to be initially activated (see FIG. 5d and Supplemental Video S4). When a root node of a branch with high branching ratios $r = 4$ or $r = 5$ was initially activated, the activation could not spread and died out (FIG. 5e). Furthermore, activation

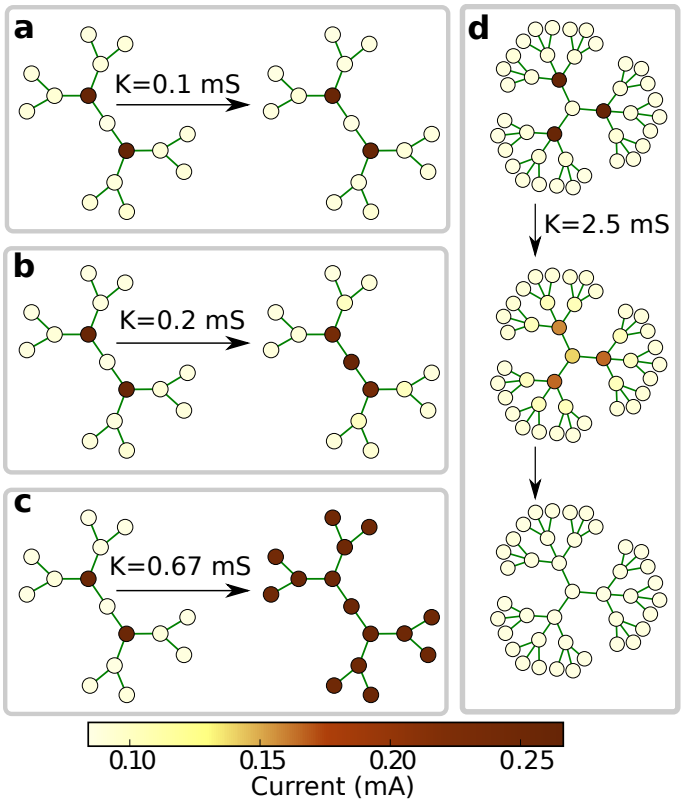


FIG. 4: Experiments with regular trees: Activation of an intermediate layer. **a,** Pinned fronts in both directions, $K = 0.10\ mS$; final state at $t = 402\ s$ is shown. **b,** Spreading front to the center and pinned front toward the periphery, $K = 0.20\ mS$, at $t = 602\ s$. **c,** Spreading fronts in both directions, $K = 0.67\ mS$, at $t = 538\ s$. **d,** A spreading front towards center and a retreating front from periphery, $K = 2.5\ mS$. Middle snapshot at $t = 25\ s$ and final state at $t = 50\ s$. $V = 1300mV$; the same color coding as in FIG. 3.

of more central node in the branch with $r = 3$ resulted in a pinned front (FIG. 5f).

## IV. DISCUSSION

We have experimentally demonstrated that bistable tree networks can support a rich variety of stationary domain patterns, determined both by the network architecture and initial activation conditions. A surprisingly good agreement with theoretical predictions has been found despite the fact that our experimental system did not perfectly meet the idealizations made in the theory [30], i.e. the state of a network element was described by more than a single variable and coupling between the elements was local, but not exactly of the diffusive form. This indicates that the considered behavior is generic and robust; therefore it can be expected in various natural and engineered bistable networks with tree-like structure, such as, e.g., nephrons of the kidney [33] or supercomputer networks [34].

While only (regular or non-regular) tree networks were considered, our results are also relevant for large random networks. Indeed, it is known [35] that locally such networks possess the tree structure. Hence, formation of stationary domains should also be characteristic for random networks provided that such domains remain sufficiently small. Finally, it should be noted that, as has been theoretically shown [31], self-organized stationary domains can be controlled by introducing global feedbacks and experimental realization of such control would further facilitate the design of complex stationary structures on networks.

### Acknowledgments

N. E. K. acknowledge financial support by the LASAGNE (Contract No.318132) and MULTIPLEX (Contract No.317532) EU projects. M. S. and I. Z. K. acknowledge support from National Science Foundation CHE-1465013.

[1] W. Horsthemke, K. Lam and P. K. Moore, Network topology and Turing instabilities in small arrays of diffusively coupled reactors, *Phys. Lett. A* **328**, 444–451 (2004).
[2] M. Karlsson, K. Sott, M. Davidson, A-S. Cans, P. Linderholm and D. Chiu, Formation of geometrically complex lipid nanotube-vesicle networks of higher-order topologies, *Proc. Natl. Acad. Sci. USA* **99**, 11573–11578 (2002).
[3] M. Wickramasinghe and I. Z. Kiss, Spatially Organized Dynamical States in Chemical Oscillator Networks: Synchronization, Dynamical Differentiation, and Chimera Patterns, *PloS ONE* **8**, e80586 (2013).
[4] L. R. Varshney, *et al.*, Structural Properties of the Caenorhabditis elegans Neuronal Network, *PLoS Computational Biology* **7**, e1001066 (2011).
[5] F. Dörfler, M. Chertkov and F. Bullo, Synchronization in complex oscillator networks and smart grids, *Proc. Natl. Acad. Sci. USA* **110**, 2005–2010 (2013).
[6] B. Ravoori, A. B. Cohen, J. Sun, A. E. Motter, T. E. Murphy and R. Roy, Robustness of Optimal Synchronization in Real Networks, *Phys. Rev. Lett.* **107**, 034102 (2011).
[7] M. E. J. Newman, The structure and function of complex networks, *SIAM Rev.* **45**, 167 (2003).
[8] A. Arenas, *et al.*, Synchronization in complex networks, *Phys. Rep.* **469**, 93–153 (2008).
[9] M. R. Tinsley,S. Nkomo and K. Showalter, Chimera and phase-cluster states in populations of coupled chemical oscillators, *Nature Phys.* **8**, 1–4 (2012).
[10] H. Nakao and A. S. Mikhailov, Turing patterns in network-organized activator–inhibitor systems, *Nature Phys.***6**, 544–550 (2010).

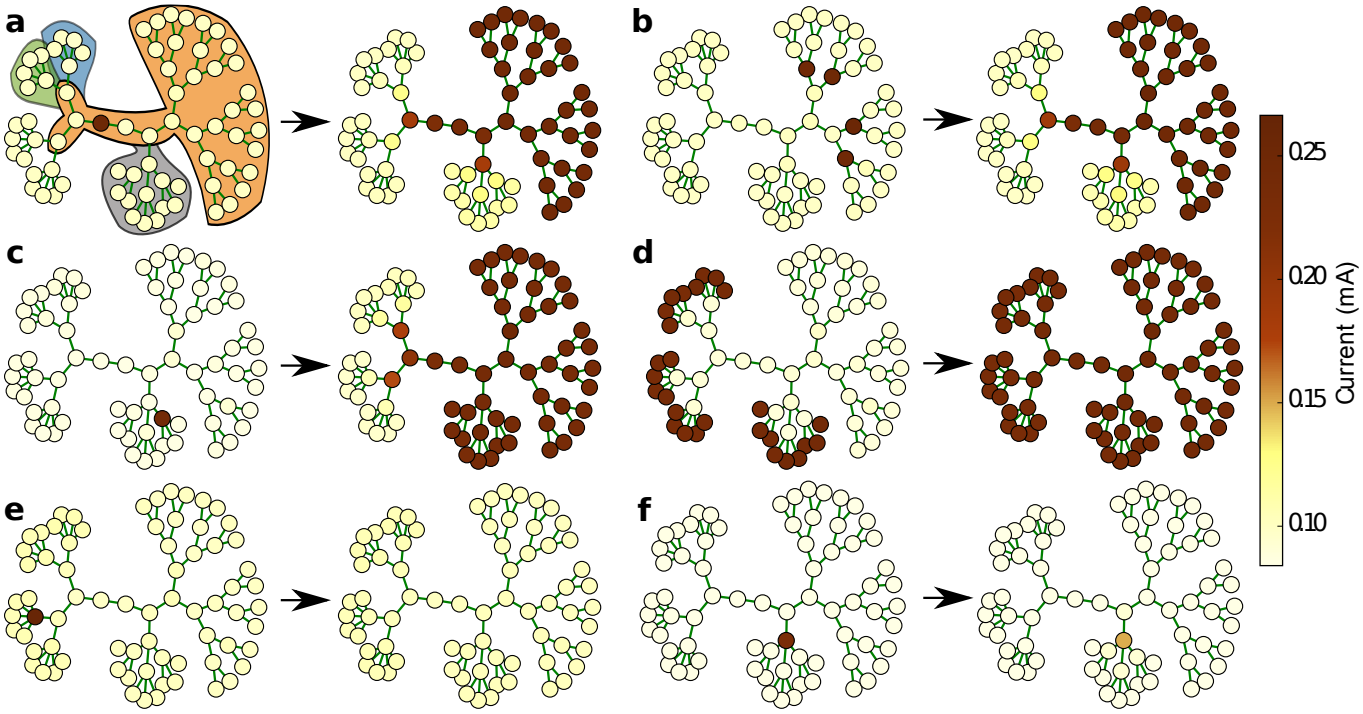


FIG. 5: Experiments with a non-regular tree. **a,** Activation of a single node from the linear chain yields spreading fronts that activate the domain $A$ ($V = 1300\ mV$, final state at $t = 654\ s$). **b,** Intermediate activation of four nodes in the domain $A$ with $r = 2$ yields spreading fronts to activate the domain $A$ ($V = 1295\ mV$, final state at $t = 241\ s$). **c,** Near periphery activation of a single node in the branch with $r = 3$ yields spreading fronts which activate the domains $A \cup B$ ($V = 1275\ mV$, final state at $t = 336\ s$). **d,** Periphery activation of the branches with $r = 3,\ 4$, and 5 yields spreading fronts to complete network activation ($V = 1280\ mV$, final state at $t = 201\ s$). **e,** Activation of a single node in the branch with $r = 5$ yields retreating fronts to complete network passivation ($V = 1300\ mV$, final state at $t = 54\ s$). **f,** Activation of a single more central node in the branch with $r = 3$ yields pinned fronts ($V = 1270\ mV$, final state at $t = 801\ s$). All experiments performed at $K = 1.3\ mS$; the same color coding as in FIG. 3.


[11] M. Wolfrum, The Turing bifurcation in network systems: Collective patterns and single differentiated nodes, *Physica D: Nonlinear Phenomena* **241**, 1351–1357 (2012).

[12] N. E. Kouvaris, S. Hata and A. Díaz-Guilera, Pattern formation in multiplex networks, *Sci. Rep.* **5**, 10840 (2015).

[13] S. Hata, H. Nakao, and A. S. Mikhailov, Dispersal-induced destabilization of metapopulations and oscillatory Turing patterns in ecological networks, *Sci. Rep.* **4**, 3585 (2014).

[14] M. Asllani, J. D. Challenger, F. S. Pavone, L. Sacconi and D. Fanelli, The theory of pattern formation on directed networks, *Nat. Commun.* **5**, 4517 (2014).

[15] N. E. Kouvaris, T. Isele, A. S. Mikhailov and E. Schöll Propagation failure of excitation waves on trees and random networks, *Europhys. Lett.* **106**, 68001 (2014).

[16] T. Isele and E. Schöll, Effect of small-world topology on wave propagation on networks of excitable elements, *New J. Phys.* **17**, 023058 (2015).

[17] A. J. Steele, M. Tinsley and K. Showalter Spatiotemporal dynamics of networks of excitable nodes, *Chaos* **16**, 015110 (2006).

[18] A. M. Turing, The chemical basis of Morphogenesis, *Philos. Trans. R. Soc.* **237**, 37 (1952).

[19] J. Horvath, I. Szalai and P. De Kepper An Experimental Design Method Leading to Chemical Turing Patterns, *Science* **324**, 772–775 (2009).

[20] N. Tompkins, *et al.*, Testing Turing's theory of morphogenesis in chemical cells, *Proc. Natl. Acad. Sci. USA* **111**, 4397–4402 (2014).

[21] Epstein, I. R. and Pojman, J. A., An Introduction to Nonlinear Chemical Dynamics: Oscillations, Waves, Patterns, and Chaos. Oxford University Press (1998).

[22] T. G. W. Graham, S. M. Ali Tabei, A. R. Dinner, and I. Rebay, Modeling bistable cell-fate choices in the Drosophila eye: qualitative and quantitative perspectives, *Development* **137**, 2265–2278 (2010).

[23] C. J. Tessone and R. Toral, System size stochastic resonance in a model for opinion formation, *Physica A* **351**, 106–116 (2005).

[24] K. Ikeda, H. Daido and O. Akimoto, Optical Turbulence: Chaotic Behavior of Transmitted Light from a Ring Cavity, *Phys. Rev. Lett.* **45**, 709 (1980).

[25] A. S. Mikhailov, Foundations of Synergetics I: Distributed Active Systems (Springer, Berlin 1990)

[26] V. Booth and T. Erneux, Mechanism for propagation failure in discrete reaction-diffusion systems, *Physica D* **188**, 206–209 (1992).

[27] T. Erneux and G. Nicolis, Propagating waves in discrete bistable reaction-diffusion systems, *Physica D* **67**, 237–244 (1993).

[28] I. Mitkov, K. Kladko and J. Pearson, Tunable Pinning of Burst Waves in Extended Systems with Discrete Sources,

*Phys. Rev. Lett.* **81**, 5453–5456 (1998).

[29] L. P. Laplante and T. Erneux Propagation failure and multiple steady states in an array of diffusion coupled flow reactors, *Physica A* **188**, 89–98 (1992).

[30] N. E. Kouvaris, H. Kori and A. S. Mikhailov, Traveling and Pinned Fronts in Bistable Reaction-Diffusion Systems on Networks, *PLoS ONE* **7**,e45029 (2012).

[31] N. E. Kouvaris and A. S. Mikhailov, Feedback-induced stationary localized patterns in networks of diffusively coupled bistable elements, *Europhys. Lett.* **102**, 16003 (2013).

[32] F. Schlögl, Chemical reaction models for non-equilibrium phase transitions, *Z. Physik* **253**, 147 (1972).

[33] D. D. Postnov, D. E. Postnov, D. J. Marsh, N. H. Holstein-Rathlou and O. V. Sosnovtseva, Dynamics of Nephron-Vascular Network. *Bull Math Biol* **74**, 2820–2841 (2012).

[34] J. R. Goodman and C. H. Sequin, Hypertree: A Multiprocessor Interconnection Topology, *IEEE Trans. Comp.* **C-30**, 923–933 (1981).

[35] A. Barrat, M. Barthélemy and A. Vespignani, *Dynamical Processes on Complex Networks*(Cambridge Univ.Press, 2008).